Manuscript submitted to
AIMS' Journals
Volume **X**, Number **0X**, XX **200X**

Website: http://AIMsciences.org

pp. **X–XX**

GAS FLOW IN PIPELINE NETWORKS

Mapundi K. Banda

University of KwaZulu-Natal
School of Mathematical Sciences
Private Bag X01
3209 Pietermaritzburg, South-Africa

Michael Herty

Technische Universität Kaiserslautern
Fachbereich Mathematik
Postfach 3049
D-67653 Kaiserslautern, Germany

Axel Klar

Technische Universität Kaiserslautern
Fachbereich Mathematik
Postfach 3049
D-67653 Kaiserslautern, Germany

(Communicated by Aim Sciences)

Abstract. We introduce a model for gas flow in pipeline networks based on the isothermal Euler equations. We model the intersection of multiple pipes by posing an additional assumption on the pressure at the interface. We give a method to obtain solutions to the gas network problem and present numerical results for sample networks.

1. **Introduction.** There has been intense research on gas networks in the past and several models for transient flow in gas pipelines have been proposed, e.g. [20, 3, 9, 24] and publications by the Pipeline Simulation Interest Group (PSIG [19]). Numerical methods have been proposed [25, 11] for simulations of the various models. Our starting point for describing transient gas flow are the isothermal Euler equations [21, 9, 16]. Using the properties of solutions to Riemann problems for those equations, we derive coupling conditions for intersections of multiple pipes, see below. Here, we do not consider further elements of gas networks like compressors. They will be considered in future work concentrating on optimization procedures for gas networks.

The isothermal Euler equation is a 2x2 system of conservation laws. Recently there has been intense research and progress in the theoretical investigations of coupling conditions for such systems. For traffic flow models the first results concerning only scalar conservation laws are due to [8, 5] and then for the 2x2 Aw–Rascle model

2000 *Mathematics Subject Classification.* Primary: 76N15; Secondary: , 35Lxx.

Key words and phrases. Isothermal Euler equation, Networks, Gas Flow.

This work was supported by the University of Kaiserslautern Excellence Cluster Dependable Adaptive Systems and Mathematical Modelling and the University of KwaZulu-Natal competitive research grant (2005) Flow Models with Source Terms, Scientific Computing, Optimization in Applications.

of traffic flow due to [10, 12]. The idea is to discuss (half-)Riemann problems at the intersections which are used to define solutions for a network problem. Additional conditions have to be posed to obtain unique solutions, see again [10, 12]. For gas dynamics we obtain the conditions by applying a similar modelling as in the engineering community [18, 6, 24, 21, 9, 19] and the references therein. Alternatives to the proposed modelling are discussed in [2] but only for a particular case not including multiple pipe intersections, like tee fittings.

2. **The Isothermal Euler equations.** The isothermal Euler equations are a simplification of the Euler equations. They are obtained from the isentropic equations which in turn are derived from the Euler equations under the assumption that the energy equation is redundant. In the isothermal Euler equations the temperature is constant.

$$p = \frac{Z\mathcal{R}T}{M_g}\rho, \tag{1}$$

where p is the pressure, Z is the natural gas compressibility factor, $\mathcal{R}$ the universal gas constant, T the absolute gas temperature, M_g is the gas molecular weight and ρ the density.

For the gas networks we assume that the isothermal Euler equations govern the dynamics inside each pipe. To keep the presentation simple, but still complex enough to model real–world applications [17, 9, 23], we assume from here on: there is negligible wall expansion or contraction under pressure loads; i.e. pipes have constant cross-sectional area. All pipes have the same diameter D. The constant $a^2 = Z\mathcal{R}T/M_g$, i.e., the sound speed, is the same for all pipes in the network. In all pipes we assume steady state friction [17, 25]. The friction factor f_g is calculated using Chen's equation [4]:

$$\frac{1}{\sqrt{f_g}} := -2\log\Big(\frac{\varepsilon/D}{3.7065} - \frac{5.0452}{N_{Re}}\log\big(\frac{1}{2.8257}\big(\frac{\varepsilon}{D}\big)^{1.1098} + \frac{5.8506}{0.8981 N_{Re}}\big)\Big) \tag{2}$$

where N_{Re} is the Reynolds number $N_{Re} = \rho u D/\mu$, μ the gas dynamic viscosity and ϵ the pipeline roughness, which are again assumed to be the same for all pipes.

Finally, the equations under consideration read

$$\partial_t \rho_j + \partial_x(\rho_j u_j) = 0, \tag{3a}$$

$$\partial_t(\rho_j\ u_j) + \partial_x(\rho_j\ u_j^2 + a^2\rho_j) = -f_g\ \frac{\rho_j\ u_j|\rho_j\ u_j|}{2D\rho_j}. \tag{3b}$$

Here, u_j denotes the velocity of a gas and $\rho_j u_j (=: q_j)$ is the flux in pipe j. The first equation is the conservation of mass and the second states the conservation of moment.

We present coupling conditions for pipe–pipe intersections in the subsequent sections. This yields a modelling of major parts of gas networks [23]. The modelling of pipe–pipe intersections is similar to the approaches in the engineering community, i.e., by assuming a constant and equal pressure inside each fitting, see below and [18, 6, 9]. For simplicity, we assume that friction is negligible near and inside pipe intersections and present only inside each pipe.

3. **Modelling of pipeline elements.** We will use the following notation throughout the remaining sections,

$$q := \rho u,\ U := \begin{pmatrix}\rho\\ q\end{pmatrix},\ F(U) := \begin{pmatrix} q\\ q^2/\rho + a^2\rho\end{pmatrix}. \tag{4}$$

Before we discuss a network of pipes, we introduce two main assumptions, that simplify the discussion following:

$$\textbf{A1}\quad \text{There are no vacuum states present, i.e., } \rho_j > 0. \tag{5}$$

$$\textbf{A2}\quad \text{The direction of flow does not change, i.e., } u_j \geq 0. \tag{6}$$

Due to assumption (6) we model a network of pipes as a directed, finite graph $(\mathcal{J}, \mathcal{V})$ and in addition we may connect edges tending to infinity. Each edge $j \in \mathcal{J}$ corresponds to a pipe. Each pipe j is modelled by an interval $[x_j^a, x_j^b]$. For edges ingoing or outgoing to the network we have $x_j^a = -\infty$ or $x_j^b = +\infty$, respectively. Each vertex $v \in \mathcal{V}$ corresponds to an intersection of pipes. For a fixed vertex $v \in \mathcal{V}$ we denote by δ_v^- (δ_v^+) the set of all indices of edges $j \in \mathcal{J}$ ingoing (outgoing) to the vertex v. On each edge $j \in \mathcal{J}$ we assume that the dynamics is governed by the isothermal Euler equations (3) for all $x \in [x_j^a, x_j^b]$ and $t \in [0, T]$ and supplemented with initial data U_j^0.

At each vertex $v \in \mathcal{V}$ we have to couple systems of the type (3) by suitable coupling conditions. To this end we introduce "intermediate" states at the vertex, similar to the constructions given in [10, 12, 13, 2]. We have one intermediate state for each connecting pipe and those states have to satisfy the coupling conditions at the vertex. To be more precise: consider a single vertex v with ingoing pipes $j \in \delta_v^-$ and outgoing pipes $j \in \delta_v^+$. Assume constant initial data U_j^0 given on each pipe. A family of functions $(U_j)_{j \in \delta_v^- \cup \delta_v^+}$ is called a solution at the vertex, provided that U_j is a weak entropic solution on the pipe j and (for U_j sufficiently regular)

$$\sum_{j \in \delta_v^-} q_j(x_j^b -, t) = \sum_{j \in \delta_v^+} q_j(x_j^a +, t) \ \forall t > 0. \tag{7}$$

This condition resembles Kirchoff's law and is referred to as Rankine-Hugoniot condition at the vertex. It imposes the conservation of mass at the intersection. We need to introduce (half-)Riemann problems and the notion of demand and supply functions to describe solutions at pipe intersections.

At a fixed junction $v \in \mathcal{V}$ we consider the (half-)Riemann problems for a pipe j,

$$\partial_t U_j + \partial_x F(U_j) = 0, \tag{8a}$$

$$U_j(x,0) = \begin{cases} U_j^0 & x < x_j^b \\ \bar{U}_j & x \geq x_j^b \end{cases} \quad j \in \delta_v^-, \tag{8b}$$

$$U_j(x,0) = \begin{cases} \bar{U}_j & x < x_j^a \\ U_j^0 & x \geq x_j^a \end{cases} \quad j \in \delta_v^+. \tag{8c}$$

Note that depending on the pipe, only one of the Riemann data is defined for $t = 0$. Later on, we construct an solution $(U_j)_j$ such that all generated waves have non-positive ($j \in \delta_v^-$) or non-negative ($j \in \delta_v^+$) speed and such that additionally the coupling condition (7) is satisfied.

We recall some mathematical properties of the isentropic Euler equations. Both characteristic families are genuine nonlinear for $\rho_j > 0$. The eigenvalues are $\lambda^{1,2}(U) = q/\rho \mp a$. We follow the standard theory [7] and notation: Consider a Riemann problem for (8a,4), i.e., an Cauchy problem for (8a) with piecewise constant initial data $U_j^0(x)$ having at most one discontinuity at $x = 0$. We consider the wave curves in the $(\rho, q)-$plane. Note that the $i-$(Lax-)shock curve and the $i-$rarefaction wave curve through a given left state $\tilde{U}$ do not coincide. They are connected smoothly in $\tilde{U}$ up to the second derivative and sketched in Figure 1. A parametrization of

the i-shock and i-rarefaction wave curve can be found for example in [16]. We will refer to the composition of the i-(Lax-)shock curve and the i-rarefaction wave curve through a given state $\tilde{U}$ shortly as $i-$*wave curve*. The $1-$wave curve is concave and intersects $\{(\rho, 0) : \rho > 0\}$ exactly once. Similarly, the $2-$wave curve is convex and also intersects $\{(\rho, 0) : \rho > 0\}$ exactly once. We refer to [7, 16] for more details.

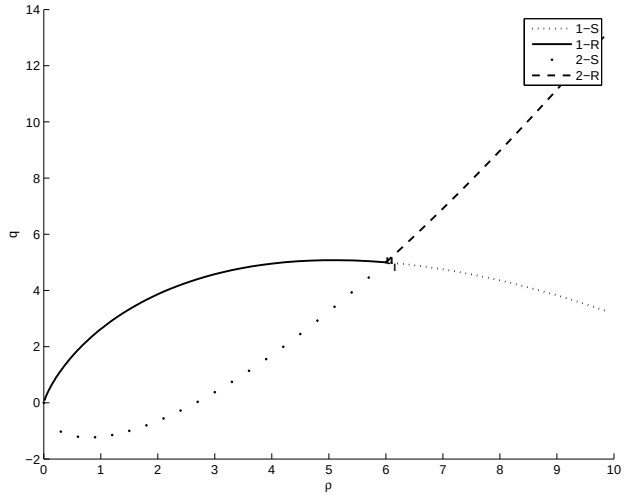

FIGURE 1. 1- and 2-wave curves through the left given state U_l.

We introduce the notion of demand and supply functions similar to [12, 15] and depending on a given (left) initial datum U_l: We consider the (convex) $1-$wave curve in the (ρ, q)-plane and define a demand function $\rho \to d(\rho; U_l)$ as an extension of the non–decreasing part of the 1–wave curve, i.e., the curve defined by $\{(\rho, q) : (\rho, q)$ can be connected to the left state U_l by either a 1–(Lax-)shock or a 1–rarefaction wave $\}$, c.f. Figure 2.

Similarly, the supply function $\rho \to s(\rho; U_l)$ is an extension to the non–increasing part of 1–wave curve through a right state U_l. Using this notion it is possible to define the admissible states $\bar{U}_j$ for given left (or right) state. We refer to [2] for details on the proofs of the following propositions.

Proposition 1. *Consider an ingoing pipe $j \in \delta_v^-$ and given constant initial data $U_j^0 =: U_l$. Denote by $d(\rho; U_l)$ the demand function.*

Then, for any given flux q^* with

$$0 \le q^* \le d(\rho_l; U_l), \tag{9}$$

there exists a unique state $\bar{U}_j =: U_r$ with $\rho_r > 0$ and $q_r = q^*$ such that the (half-)Riemann problem (8a,8b) admits a solution which is either constant or consists of waves with negative speed only.

The state $\bar{U}_j$ is called an admissible state for the left initial U_l.

The proof of this proposition can be obtained by considering states $\bar{U}_j, \bar{\rho}_j, \bar{q}_j \ge 0$ on the 1-(Lax-)shock curve (or the 1–rarefaction curve) through U_l, which can be connected to $U_l \equiv U_j^0$ by a wave of non–positive speed. It is easy to see, that all those states have the property $\bar{q}_j \le d(\rho_l; U_l)$. Furthermore, if a state $\bar{U}_j$ is connected

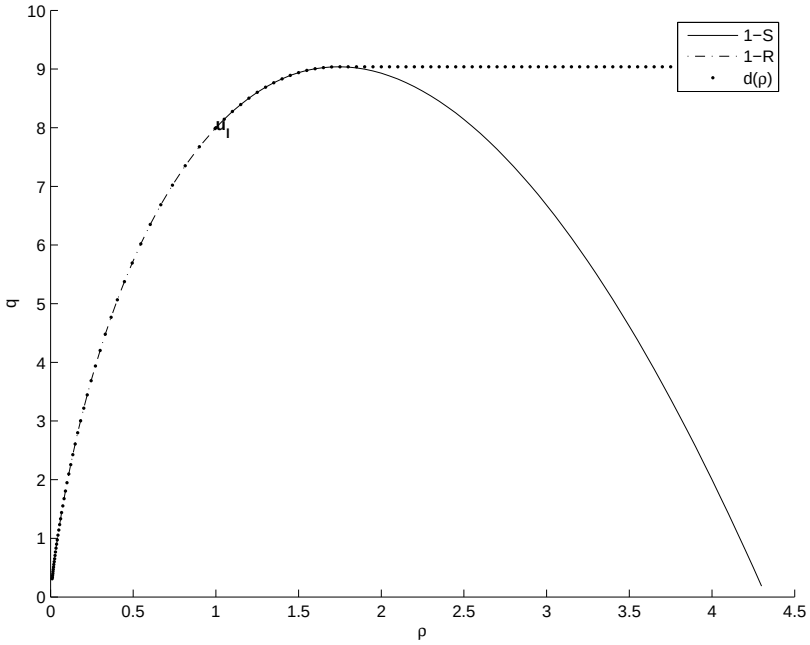

FIGURE 2. Demand function $\rho \to d(\rho; U_l)$ for a given left state U_l and its 1–wave curve.

to U_l such that the associated wave is of the second family, we always obtain a non–negative speed of this wave. Therefore, states $\bar{U}_j$ on the 2–wave curve are *not* admissible.

Proposition 2. *Consider constant initial data $U_j^0 =: U_r$ with $\rho_r > 0$ and $q_r \geq 0$ and an outgoing pipe $j \in \delta_v^+$.*

Then the (half-)Riemann problem (8a, 8c) with $\bar{U}_j =: U_l$ and $\rho_l > 0$, $q_l \geq 0$ admits either the constant solution $U_l \equiv U_r$ or the solution is a juxtaposition of waves of positive speed provided that

$$0 \leq q_l \leq s(\rho_m; U_m) \tag{10}$$

for an arbitrary state $U_m \equiv (\rho_m, q_m)$ with the properties

$$\tilde{\rho} \leq \rho_m < \infty \text{ and} \tag{11a}$$

$$U_m \text{ is either on the 2-rarefaction or} \tag{11b}$$

$$\text{on the 2-(Lax-)shock wave curve through (right) } U_r, \tag{11c}$$

where $\tilde{\rho}$ is the zero of the function

$$q(\rho) := \rho \frac{q_r}{\rho_r} + a\rho \log\left(\frac{\rho}{\rho_r}\right) \tag{12}$$

in the interval $[\rho_r \exp\left(-\frac{q_r}{\rho_r a} - 1\right), \rho_r]$.

The state $\bar{U}_j$ is called admissible state for the right initial data U_r.

Here, slightly more analysis is involved due to the possibility of solutions U_j consisting of a juxtaposition of 1– and 2–waves. Again, we refer for the details

to [2] and recall only the basic idea: We start by assuming a given intermediate point U_m. Then, by a similar reasoning as in (1) we find points $\bar{U}_j$ which can be connected to the (right) state U_m by a wave of the first family of non–negative speed. Those points $\bar{U}_j$ then have a flux $\bar{q}_j \leq s(\rho_m; U_m)$, i.e., (10). To obtain an admissible solutions the intermediate points U_m have to be connected to the right state $U_r \equiv U_j^0$ by a wave of the second family, (11b,11c). There is no restriction here, since all those waves have non–negative speed. The only crucial point is to satisfy assumption (6), namely, all states have to have a non–negative flux: Recall that $\{\rho, q(\rho)\}$ with $q(\rho)$ given by (11c) is a parametrization of the 2–rarefaction wave curve through the right state U_r and therefore, condition (11a) ensures that U_m has a non–negative flux q_m.

We model the intersections of pipes by defining additional coupling conditions to (7). In [2] different possibilities were introduced and also the case $a_j \neq a_{j'}$ was treated. As mentioned in Remark 3.2 [2], real–world applications usually assume constant pressure $a^2\rho$ inside each vertex, i.e., inside each pipe–to–pipe fitting. Depending on the geometry, the pressure at the vertex is reduced by so–called "minor losses " [6]. This can be modelled by a known pressure drop factor f_{ext} depending on the flow and density near the intersection [18, 6]. Furthermore, the existence of minor losses implies that in general the moment $q_j/\rho_j + a^2\rho_j$ is *not* conserved at the intersection. As a simplification we assume in the following that there are no minor losses: For all $j, j' \in \delta_v^+ \cup \delta_v^-$:

A3 The pressure at the vertex is a constant, i.e., $a^2\rho_j = a^2\rho_{j'}$. (13)

The simplest possible situation consist of just two pipes and constant initial data. Let's assume the pipes are connected at $x_1^b = x_2^a$. Then, the following proposition guarantees the existence of a solution satisfying (5), (6) and (13).

Proposition 3. *Consider a single intersection v with an ingoing pipe $j = 1 \in \delta_v^-$ an outgoing pipe $j = 2 \in \delta_v^+$. Assume constant initial data U_j^0 with $\rho_j^0 > 0$ and $q_j \geq 0$ for $j = 1, 2$. Assume that*

$$\tilde{\rho} \leq \tilde{\tilde{\rho}}, \tag{14}$$

where $\tilde{\rho}$ is as in Proposition 2 and $\tilde{\tilde{\rho}}$ is the zero of the 1-(Lax-)shock wave curve through the left state U_1^0.

Then there exists a unique solution $U_j(x,t), j = 1, 2$ with the following properties

1. *U_j is a weak entropic solution to (8a, 4) with $U_j(x, 0) = U_j^0$.*
2. *Equation (7) is satisfied for all times $t > 0$, i.e., $q_1(x_1^b, t) = q_2(x_2^a, t)$.*
3. *Condition (13) is satisfied for all times $t > 0$, i.e., $a^2\rho_1(x_1^b, t) = a^2\rho_2(x_2^a, t)$.*
4. *The flux at the interface $q_1(x_1^b, t)$ is maximal subject to the other conditions (1)-(3) being satisfied.*

Proof. The proof is similar to Theorem 3.1 [2] but given for sake of completeness. Due to assumption (14) there exists a unique point U_m obtained as intersection of following two curves in the (ρ, q)-plane: The 2–wave curve through the right state U_2^0 intersects the 1–wave curve through the left state U_1^0. Furthermore, U_m is such that $\rho_m > 0$ and $q_m \geq 0$. Let $\tilde{q}$ be the flux at the interface defined by $\tilde{q} := \min\{d(\rho_1^0; U_1^0), s(\rho_m; U_m)\}$. Then, due to Proposition 1 and 2, there exists $\bar{U}_1$ and $\bar{U}_2$ respectively, such that the solution U_1 to (8a,8b) and the solution U_2 to (8a,8c) consists of waves only of negative and positive velocity, respectively: Indeed, with the other cases being similar, we discuss the following case in detail: Assume that $\tilde{q} = d(\rho_1^0; U_1^0) > q_1^0$. Then, $\bar{U}_1 = (\tilde{q}/a, \tilde{q})$. Therefore, $\bar{U}_1$ is connected to

$U_l := U_1^0$ by a 1–rarefaction wave of negative speed. Now, we turn to the outgoing road $j = 2$. By assumption $s(\rho_m; U_m) \geq \tilde{q}$ and using Proposition (2) there exists a state $\bar{U}_2$ such that $\bar{q}_2 = \tilde{q}$ and such that $\bar{U}_2$ can be connected to the right state U_m by a 1–wave of non–negative speed. Furthermore, by construction, U_m can be connected to $U_r := U_2^0$ by a 2–wave of non–negative speed. Moreover, $\bar{U}_2 \equiv \bar{U}_1$, since $\bar{U}_2$ belongs also to the 1–rarefaction wave curve through the left state U_1^0 and since both have the same flux $\tilde{q}$. This finally yields (13). □

Remark 1. For the discussion later on, we remark, that the key step in defining $U_j(x,t)$ is the solvability of the maximization problem (15).

$$\max \tilde{q} \qquad \text{subject to} \tag{15a}$$
$$0 \leq \tilde{q} \leq d(\rho_1^0; U_1^0) \qquad \text{and} \tag{15b}$$
$$0 \leq \tilde{q} \leq s(\varrho_m^2; U_m^2) \qquad \text{and} \tag{15c}$$
$$\varrho^1 = \varrho^2, \tag{15d}$$

Herein, U_m^2 is the intersection of the 1-wave curve through U_1^0 and the 2-wave curve through U_2^0; ϱ^j is implicitly defined such that $(\varrho^1, \tilde{q})$ is admissible for the left state U_1^0 and $(\varrho^2, \tilde{q})$ is such that it can be connected by a 1–wave of positive speed to the right state U_m.

We can also define solutions to (8a), (4) as the restriction of the entropic solution $U^* = (\rho^*, q^*)$ to the Riemann problem

$$U_t^* + F(U^*)_x = 0,\ U^*(x,0) = \begin{cases} U_1^0 & x < x_1^b = x_2^a \\ U_2^0 & x > x_1^b \end{cases} . \tag{16}$$

i.e. $U_1 := U^*$ for $x < x_1^b$ and $U_2 := U^*$ for $x > x_2^a$. Both, the one given above and the solutions according to Proposition 3, *coincide* provided that $\rho^*(x,t) > 0$ and $u^*(x,t) = q^*(x,t)/\rho^*(x,t) \geq 0$. In the case $u^* < 0$ the assumption (14) is violated. Furthermore the approach of Proposition 3 can be extended to intersections of more than two pipes.

Remark 2. In the special situation of pipe–to–pipe fittings of Proposition 3 the moment $q^2/\rho + a^2\rho$ is conserved. However, this is not true in the case of pipe intersections discussed below, c.f. Remark 3.

Besides pipe–to–pipe connections a typical network contains tees, as for example depicted in Figure 3. In contrast to [2], we model multiple pipe intersections under the assumption (13). This yields a far more complex problem and there does not exist a solution in the general case. We present a construction for suboptimal solutions to the problem and numerical results for pipe networks.

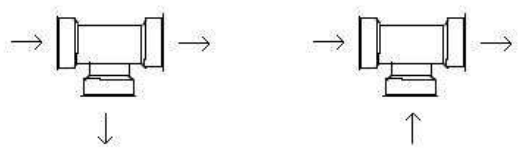

FIGURE 3. Two types of tees. The arrows indicate the direction of the flow. The left and right are referred to as type A and B, respectively.

Formally, we proceed as above to define a solution for the tee type intersections: For an intersection v of type A we set $j = 1 \in \delta_v^-$ and $j = 2, 3 \in \delta_v^+$ and for type B $j = 1, 2 \in \delta_v^-$ and $j = 3 \in \delta_v^+$, respectively. We consider constant initial data $U_j^0 = (\rho_j^0, q_j^0)$ where $\rho_j^0 > 0$ and $q_j^0 \geq 0$ for $j = 1, 2, 3$. Analogously to Proposition 14 we are looking for weak entropic solutions $U_j(x, t)$ to (8a,4) that additionally satisfy the coupling conditions:

Definition 1. Consider a tee intersection v of type A or B, with $\delta_v^\pm$ as above and constant initial data $U_j^0, j = 1, 2, 3$.

A family of functions $\{U_j\}_{j=1,2,3}$ is called solution at the tee, if for all j, U_j is a weak entropic solution to (8a,4) and if for sufficiently regular functions U_j the coupling conditions (7) and (13) are satisfied, i.e., the following holds $\forall t > 0$

$$\sum_{j \in \delta_v^-} q_j(x_j^b -, t) = \sum_{j \in \delta_v^+} q_j(x_j^a +, t), \tag{17a}$$

$$a^2 \rho_i(x_i^b -, t) = a^2 \rho_j(x_j^a +, t) \; \forall i \in \delta_v^-, j \in \delta_v^+. \tag{17b}$$

We discuss intersections of type A first. As in the proof of Proposition 3 and in Remark 1 we obtain a maximization problem for the flux $\tilde{q}_1$ at the interface:

$$\max \textstyle\sum_{j=1}^3 \tilde{q}^j \qquad \text{subject to} \tag{18a}$$

$$\tilde{q}^1 := \tilde{q}^2 + \tilde{q}^3 \leq d(\rho_0^1; U_1^0) \quad \text{and} \tag{18b}$$

$$0 \leq \tilde{q}^j \leq s(\varrho_m^j; U_m^j) \qquad j = 2, 3 \text{ and} \tag{18c}$$

$$\varrho^2 = \varrho^3 = \varrho^1. \tag{18d}$$

Since some of the formulas are implicit we discuss them in detail: Assume fixed fluxes $\tilde{q}^j \in \mathbb{R}, j = 1, 2, 3$ with $\tilde{q}^1$ being less or equal to the demand $d(\rho_0^1; U_1^0)$ of the incoming pipe. Then, $\tilde{q}^j, j = 2, 3$ are such that the construction following is possible: The state $(\varrho^1, \tilde{q}^1)$ is admissible for U_1^0, see Proposition (1) and this determines ϱ^1. Then, by (18d), the states $\bar{U}_j := (\varrho^j, \tilde{q}^j), j = 2, 3$ are defined. The quantities $\varrho_m^j, j = 2, 3$ are defined implicitly: The (intermediate) state $U_m^j = (\varrho_m^j, q_m^j)$ for $j = 2, 3$ are obtained as point of intersection of the following two curves: First, the 1–wave curve through the left state $\bar{U}_j$ and second, the 2–wave curve through the right state U_2^0. This point of intersection is unique, if it exist. Finally, we assume that (18c) holds for $\tilde{q}^j$. As seen above, it is a priori not clear for which values of $\tilde{q}^j$ the construction above is possible. Let $\mathcal{Q}$ denote the set of fluxes $\mathcal{Q} := \{(\tilde{q}^j)_j, j = 1, 2, 3\}$ such that (18b) - (18d) holds, i.e., the above construction is well–defined for all points in $\mathcal{Q}$. Then, in the general case, the maximization problem (18) can have no solution, i.e., $\mathcal{Q} = \emptyset$, or multiple solutions. Again, we emphasize that there is no information on the structure of the set $\mathcal{Q}$. However, for any point $(\tilde{q}^j)_j \in \mathcal{Q}$ we can associate a weak solution $\{U_j\}_j, j = 1, 2, 3$ satisfying the coupling conditions (7) and (13): The solution U_1 on the incoming pipe is obtained as solution to (8a,8b) with $\bar{U}_1 := (\varrho^1, \tilde{q}^1)$. On each outgoing pipe $j = 2, 3$ we obtain U_j as solution to (8a, 8c) with $\bar{U}_j := (\varrho^j, \tilde{q}^j)$. Then, $\{U_j\}$ is a solution in the sense of Definition 1.

Next, we give a geometrical construction for finding at least one point belonging to the set $\mathcal{Q}$:

Consider the (ρ, q)-plane and the following two curves. First, the $1-$wave curve (C_1) through the left state U_1^0. Denote by $\tilde{\tilde{\rho}}$ the intersection point with $\{(\rho, 0) : \rho > 0\}$. Second, the curve $C_2 := \{(\rho, q^2(\rho) + q^3(\rho)\}$ where for each $j = 2, 3$ $(\rho, q^j(\rho))$ belongs to either the 2-(Lax-)shock curve or to the 2-rarefaction wave curve through

the right state U_j^0. C_2 is a convex function and let the unique intersection point with $\{(\rho, 0) : \rho > 0\}$ be denoted as $\tilde{\rho}$. If $\tilde{\rho} < \tilde{\tilde{\rho}}$, then there exists a (unique) point $U_1^* = (\rho^*, q_1^*)$ as intersection of C_1 and C_2. Assume now that U_1^* is an admissible state for the left initial datum U_1^0. Additionally assume that for $j = 2, 3$ the state $(\rho^*, q^j(\rho^*))$ is an admissible state for the right initial datum U_j^0. Note that the state $(\rho^*, q^j(\rho^*))$ belongs to the 2-wave curve through the right state U_j^0. Therefore, admissibility reduces to the condition $q^j(\rho^*) \geq 0, j = 2, 3$. Finally, the point $(q_1^*, q^2(\rho^*), q^3(\rho^*)) \in \mathcal{Q}$. We refer to Figure 4 for an example.

Remark 3. Comparing the result of the construction with coupling conditions for related systems, like the Aw–Rascle system of traffic flow, we see that we can not prescribe a flux distribution. E.g. in [10, 12] it is assumed that instead of (7) the following stronger condition holds:

$$q_j(x_j^a+, t) = \sum_{i \in \delta_v^-} \alpha_{ij} q_i(x_i^b, t),$$

where α_{ij} are percentages of drivers coming from arc i and heading to arc j. In contrast the final flux distribution for our gas network is here implicitly given by the initial data and the restriction (13).

In general a weak solution in the sense of Definition 1 does not conserve the second moment $q_j^2/\rho_j + a^2\rho_j$. Therefore it is also **not** a weak solution in the sense of [12, 13]. There weak solution at an intersection was introduced as follows: Consider a vertex $v \in \mathcal{V}$ and a set $j = 1, \ldots, \mathcal{J}$ of smooth functions $\phi_i : [0, +\infty] \times [x_j^a, x_j^b] \to \mathbb{R}^2$ having compact support in $[x_j^a, x_j^b]$. Let ϕ_j be smooth across each junction, i.e., for each pipe $i \in \delta_v^-$ and each pipe $j \in \delta_v^+$ we assume

$$\phi_i(x_i^b) = \phi_j(x_j^a), \tag{19a}$$

$$\partial_x \phi_i(x_i^b) = \partial_x \phi_j(x_j^a, t). \tag{19b}$$

Then a set of functions $U_j = (\rho_j, q_j), j = 1, \ldots, \mathcal{J}$ is called a weak solution of (8a,4), if and only if for all families of test functions ϕ_j with the property (19) equation (20) holds:

$$\sum_{j=1}^{\mathcal{J}} \int_0^\infty \int_{x_j^a}^{x_j^b} U_j \cdot \partial_t \phi_j + F(U_j) \cdot \partial_x \phi_j dx dt \tag{20a}$$

$$- \int_{x_j^a}^{x_j^b} U_j^0(x) \cdot \phi_j(x, 0) dx = 0 \tag{20b}$$

Since the solution U_j does not necessarily conserve the second moment, it is not a solution in the sense of equation (20). Again, we emphasize that Definition 1 is motivated by the discussions and observations of real–world gas networks [19, 21, 9, 18, 6].

We proceed in a similar way for the other tee intersection B. In this case $j = 1, 2 \in \delta_v^-$ and $j = 3 \in \delta_v^+$ and the corresponding maximization problem reads

$$\max \textstyle\sum_{j=1}^3 \tilde{q}^j \qquad \text{subject to} \tag{21a}$$

$$0 \leq \tilde{q}^j \leq d(\rho_j^0; U_j^0) \qquad j = 1, 2 \text{ and} \tag{21b}$$

$$\tilde{q}^3 := \tilde{q}^1 + \tilde{q}^2 \leq s(\varrho_m^3; U_m^3) \quad \text{and} \tag{21c}$$

$$\varrho^2 = \varrho^3 = \varrho^1. \tag{21d}$$

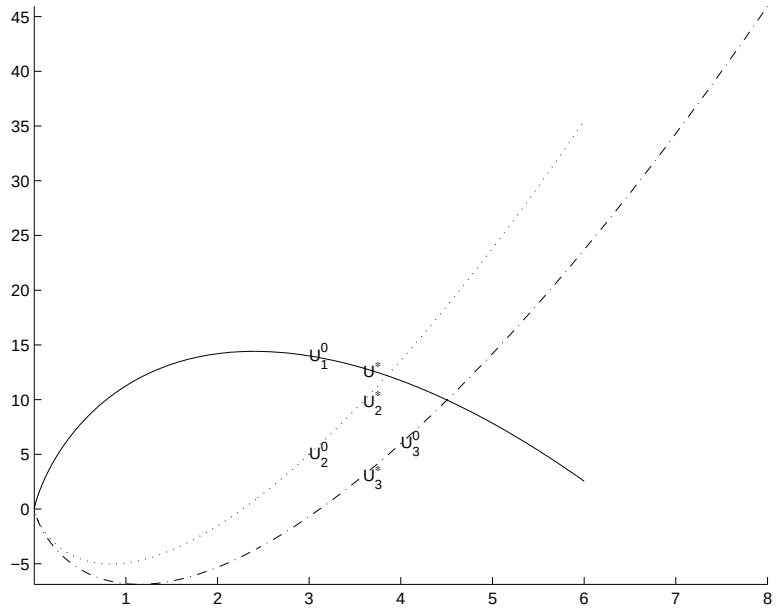

FIGURE 4. Example of states U_j^0 for a tee intersection of type A and example of the geometrical construction of a point in the set $\mathcal{Q}$ of (18). Dashed and dotted lines are 2-wave curves through the (right) state U_2^0 and U_3^0, respectively. The solid line is the 1-wave curve through (left) state U_1^0. The curve C_1 coincides with the solid line. The curve C_2 (which is not shown), is the point wise sum of the dashed and the dotted line as explained above. The intersection of C_2 and C_1 is U^* and the point $(q^*, q_2^*, q_3^*) \in \mathcal{Q}$. Therefore, the data for the (half-)Riemann problems is given by $\bar{U}_1 =: U^*$ and $\bar{U}_j =: U_j^*, j = 2, 3$, respectively. The sound speed is $a = 6$.

Assume fixed given fluxes $\tilde{q}^j, j = 1, 2, 3$ satisfying (21b) and such that the following holds. The values $\varrho^j, j = 1, 2$ are defined such that $(\varrho^j, \tilde{q}^j)$ are admissible for U_j^0, see Proposition (1), and satisfy (21d). By (21d), $\varrho^3 = \varrho^1$ and U_m^3 is defined implicitly as above. We omit the further details and give again a geometrical construction for finding at least one point $(\tilde{q}^j)_j, j = 1, 2, 3$ such that (21b-21d) holds:

Consider the following two curves in the $(\rho, q)-$plane. First, the curve C_1 is given by the 2-wave curve through the right state U_3^0. Second, the curve C_2 is given by the superposition of the 1-wave curve through the left state U_1^0 with the 1-wave curve through the left state U_2^0, i.e., $C_2 := \{(\rho, q^1(\rho) + q^2(\rho)\}$ where for $j = 1, 2$ the state (ρ, q^j) belongs to the $j-$wave curve through U_j^0. Note that C_2 is a convex curve in the (ρ, q)-plane. The point $U_m = (\rho_m, q_m)$ of the intersection of C_1 and C_2 is unique, if it exists. We assume U_m exists and, furthermore, we assume $\rho_m > 0, q_m \geq 0$. If additionally the point $(\rho_m, q^1(\rho_m))$ and the point $(\rho_m, q^2(\rho_m))$ are admissible for the left state U_1^0 and U_2^0, respectively, then $(q^j(\rho_m), q^j(\rho_m), q_m)$ satisfies (21b)-(21d). As before, we can associate a solution $\{U_j\}_j$ in the sense of Definition 1 to those flux values: For $j = 1, 2$ we solve the (half-)Riemann problems (8a,8b) with $\bar{U}_j := (\rho_m, q^j(\rho_m))$. By construction $U^* =: \bar{U}_3$ is admissible for the

right state U_3^0 and the solution U_3 to (8a,8c) is a wave of the second family only and of positive speed. Finally, due to construction the conditions (14) and (13) are satisfied, see Figure 5 for an example.

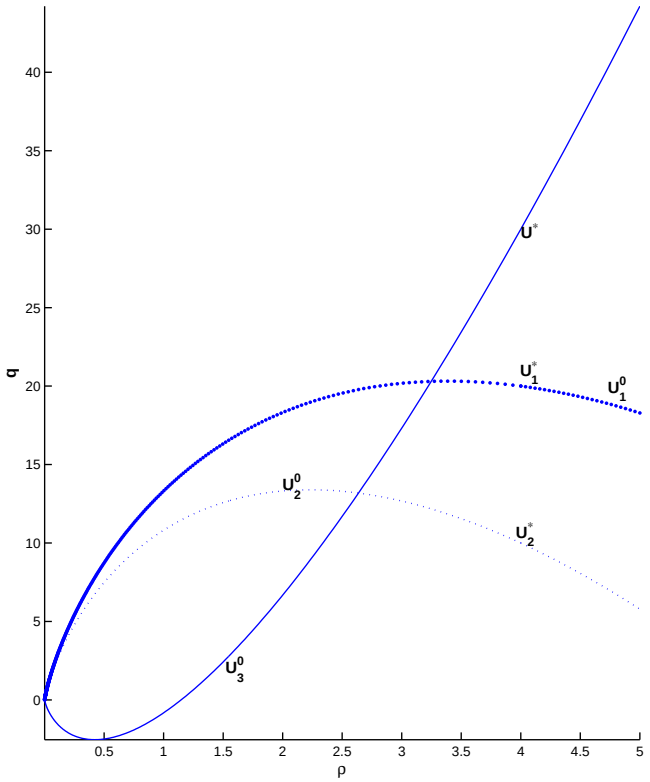

FIGURE 5. Example of states U_j^0 for a tee intersection of type B with corresponding wave curves. The intersection of C_2 and C_1 is U^*. Dashed and dotted lines are 1-wave curves through the (left) state U_1^0 and U_2^0, respectively. Solid line is the 2-wave curve through (right) state U_3^0. The data for the half-Riemann problems are $\bar{U}_j =: U_j^*$ for $j = 1, 2$ and $\bar{U}_3 =: U^*$. The sound speed is $a = 6$.

4. **Numerical Results.** We present results for the isothermal Euler equations with friction inside the pipes. The friction factor is given by equation (2). As discussed before all pipes have the same diameter D and the same sound speed a. Pipes can be connected to other pipes by tee intersections as those in Figure 3. The governing equations are (3) and the initial data is such that the (geometrical) constructions of the previous section is valid.

For the numerical results we use a relaxed scheme [14]: We apply a second order MUSCL scheme together with a second order TVD time integration scheme. Other

approaches can be similarly applied [1]. A treatment of the source term (pipe friction) is undertaken as discussed in [25]. The integration of the source term is done by solving an ordinary differential equation exactly after splitting (3). In all computations we use a space discretization of $\Delta x = 1/800$ and a time discretization Δt according to the CFL condition with CFL $= 3/4$.

Example 1: The first example is the same as discussed in Figure 4. The pipe $j = 1$ is coupled by tee intersection of type A to the pipes $j = 2$ and $j = 3$ at the points x_1^b, x_2^a and x_3^a, respectively. The discretization of the spatial domain is such that $x_1^b = 1$ and $x_2^a = x_3^a = 0$. The initial data is as in Figure 4 given by $U_1^0 = (3, 14), U_2^0 = (3, 5)$ and $U_3^0 = (4, 6)$. The sound speed is $a = 6$. ¿From the Riemann problems we expect a 1-(Lax-)shock on pipe $j = 1$, a 2-(Lax-)shock on pipe $j = 2$ and a 2-rarefaction wave on pipe $j = 3$. We give snapshots of the densities ρ_j for times $0 \le t \le 3.5$ and a contour plot of the fluxes q_j in Figure 6. We observe that our second order scheme captures well the shocks in both families. The 2-rarefaction wave can be observed in the contour plots of the flux q_3.

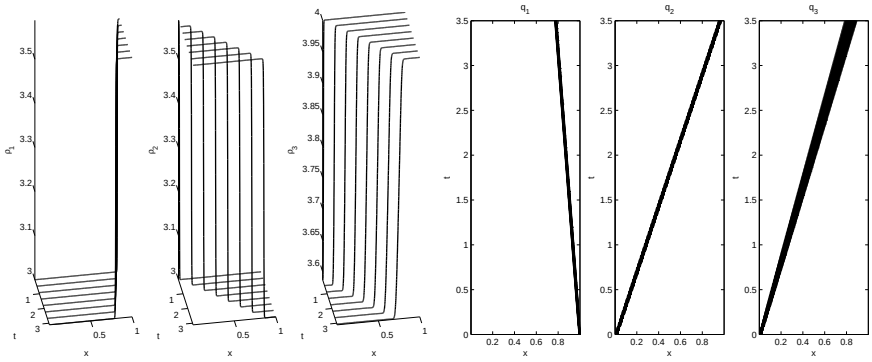

FIGURE 6. Snapshots of the densities ρ_j (left) and contour lines of the fluxes q_j (right) for three coupled pipes at a tee intersection of type A.

Example 2: The next example is the same as discussed in Figure 5. The pipes $j = 1$ and $j = 2$ are coupled by a tee intersection of type B to the pipe $j = 3$ at the points x_1^b, x_1^b and x_3^a, respectively. The discretization of the spatial domain is such that $x_1^b = x_2^b = 1$ and $x_3^a = 0$. The initial data is as in Figure 5 given by $U_1^0 = (4, 4), U_2^0 = (2, 8)$ and $U_3^0 = (2, 3)$. The sound speed is $a = 6$. ¿From the Riemann problems we expect a 1-rarefaction wave on pipe $j = 1$, a 1-(Lax-)shock on pipe $j = 2$ and a 2-(Lax)-shock on pipe $j = 3$. We give snapshots of the densities ρ_j for times $0 \le t \le 3$ and a contour plot of the fluxes q_j in Figure 7. We observe that our second order scheme captures well the shocks in both families. The 1-rarefaction wave can be observed in the contour plots of the flux q_1.

Example 3. We consider a small network for five coupled pipes with three inflows as indicate in Figure 8. We use a friction factor $f_g = 10^{-3}$ and the diameter of all pipes is $D = 10^{-1}$. The sound speed is $a = 6$, each pipe has length $L = 1$ and is discretized using $\Delta x = 1/400$.

We start with a stationary state on all pipes. Then we simulate a pressure increase and decrease on the two vertical connected pipes labelled 2 and 4, to be

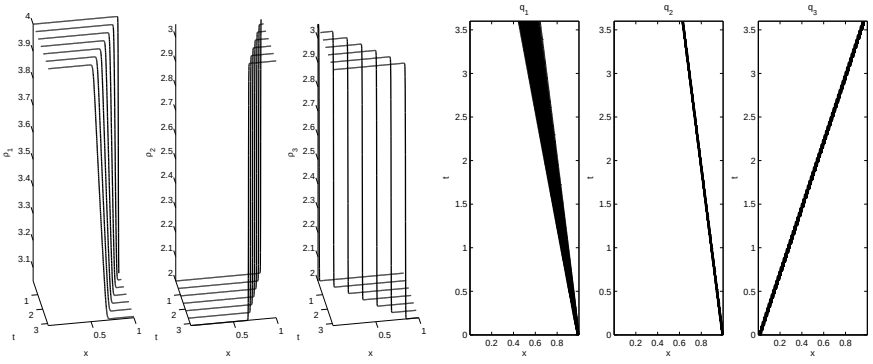

FIGURE 7. Snapshots of the densities ρ_j (left) and on contour lines of the fluxes q_j (right) for three coupled pipes at a tee intersection of type B.

more precise the initial profile are given by

$$U_2^0(x) = \begin{cases} (4 + \frac{1}{2}\sin(\pi(2x-1)), 2) & x > \frac{1}{2} \\ (4,2) & x < \frac{1}{2} \end{cases}$$

$$U_4^0(x) = \begin{cases} 4 + \frac{1}{2}\sin(4\pi(x-\frac{1}{4})), 2) & \frac{1}{2} < x < \frac{3}{4} \\ (4,2) & \text{else} \end{cases}$$

Initial conditions on pipes $1, 3, 5$ are $(4,2), (4,4), (4,6)$. The inflow on U_2 and U_4 is shifted to obtain a non–symmetric solution, see below. Contour plots of the pressure p_j and the flux q_j for the pipes $1, 3$ and 5 respectively are given in Figure 9. In this Figure pipes $1, 2$ and 3 are connected at $x = 1$ and pipes $3, 4$ are connected at $x = 2$.

We observe that the pressure is continuous through the intersections due to (13) but the flux is not. The pressure increase and decrease on pipes 2 and 4 results in two shock waves on the intermediate pipe 3 starting at $t = 0$ and $t = 1$. The waves interact inside this pipe before colliding with the pipe boundaries to the right and to the left.

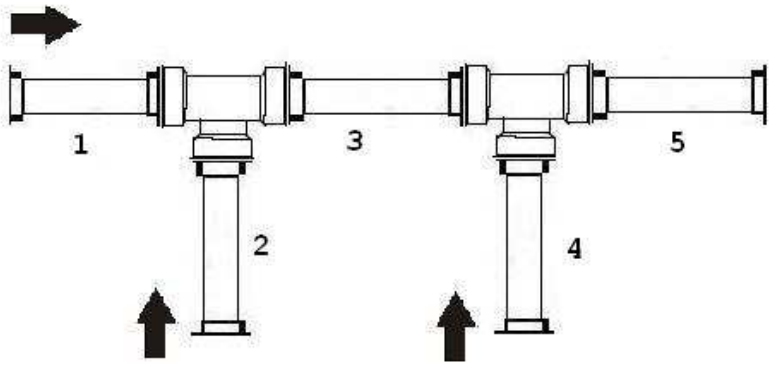

FIGURE 8. Sample network with three inflows and one outflow pipe

Example 4. Besides pipe intersection real gas networks contain valves. We model a valve as a pipe–to–pipe intersection with prescribed zero flux on the outgoing pipe. The example is similar to [25]. We consider a system of two pipes $j = 1, 2$ connected at $x_1^b = x_2^a = 1$. The initial data is $U_1^0(x) = [.15, 70]$ and $U_2^0(x) = [.15, 0]$, i.e., the valve is closed at time $t = 0$. The speed of sound is $a = 360$ and $\Delta x = 1/800$. We assume no friction inside the pipe. The evolution of the pressure $a^2\rho_j$ and the flux are shown in Figure 10. We observe the backwards moving 1-(Lax-)shock wave with increased pressure and reduced flux. As before we observe the reasonable resolution of the shock wave by our numerical scheme.

5. **Summary.** We introduced coupling conditions for the isothermal Euler equations in the case of multiple pipe connections. As necessary additional coupling condition an equal pressure assumption is imposed. This is in accordance with typical modelling approaches for gas pipelines in the engineering literature. Under this assumption we prove existence of solutions at a pipe–to–pipe intersection. We state the general problem and give a geometrical construction which allows to obtain solutions for tee intersections. We present a numerical scheme which resolves the arising shock and rarefaction waves. In the numerical results we show, how the flow in the pipe is affected by pressure drops and increases. Future work will concentrate on the optimization of gas networks including compressors and valves.

REFERENCES

[1] R. Aregba-Driollet and R. Natalini, *Discrete kinetic schemes for multidimensional conservation laws*, SIAM J. Num. Anal., 6 (2000), pp. 1973–2004.

[2] M. K. Banda and M. Herty and A. Klar, *Coupling conditions for gas networks governed by the isothermal Euler equations*, preprint (2005).

[3] K. S. Chapmann, *Virtual Pipeline System Testbed to Optimize the US Natural Gas Transmission Pipeline System*, Technology Status Assessment Report, (2002).

[4] N.H. Chen, *An explicit equation for friction factor in pipe*, Ind. Eng. Chem. Fund. (1979), pp. 296–297.

[5] G.M. Coclite and M. Garavello and B. Piccoli, *Traffic flow on a road network*, SIAM J. Math. Anal., 36, (2005), pp. 1862-1886.

[6] Crane Valve Group, *Flow of Fluids Through Valves, Fittings and Pipes*, Crane Technical Paper No. 410 (1998).

[7] C. M. Dafermos, *Hyperbolic Conservation Laws in Continuum Physics*, Springer Verlag, Berlin, (2000).

[8] H. Holden and N. H. Risebro, *A mathematical model of traffic flow on a network of unidirectional roads*, SIAM J. Math. Anal., 26 (1995), p. 999.

[9] K. Ehrhardt and M. Steinbach, *Nonlinear gas optimization in gas networks*, Modeling, Simulation and Optimization of Complex Processes (eds. H. G. Bock, E. Kostina, H. X. Pu, R. Rannacher), Springer Verlag, Berlin, (2005).

[10] M. Garavello and B. Piccoli, *Traffic flow on a road network using the Aw-Rascle model*, preprint, (2004).

[11] M. J. Heat and J. C. Blunt, *Dynamic simulation applied to the design and control of a pipeline network*, J. Inst. Gas Eng., 9 (1969), pp. 261–279.

[12] M. Herty and M. Rascle, *Coupling conditions for the Aw–Rascle equations for traffic flow*, preprint, (2005).

[13] H. Holden and N. H. Risebro, *A mathematical model of traffic flow on a network of unidirectional roads*, SIAM J. Math. Anal., 26 (1995), p. 999–1017.

[14] S. Jin and Z. Xin, *The relaxation schemes for systems of conservation laws in arbitrary space dimensions*, Comm. Pure Appl. Math., 48 (1995), pp. 235–277.

[15] J. P. Lebacque, *Les modeles macroscopiques du trafic*, Annales des Ponts., 67 (1993), pp. 24–45.

[16] R. J. LeVeque, *Numerical methods for conservation laws*, Birkhäuser Verlag, Basel, (1992).

[17] A. Martin and M. Möller and S. Moritz, *Mixed Integer Models for the stationary case of gas network optimization*, TU Darmstadt Preprint, to appear in Math. Programming (2005).
[18] F. M. White, *Fluid Mechanics*, McGraw–Hill, New York, (2002).
[19] Pipeline Simulation Interest Group, www.psig.org.
[20] A. J. Osciadacz, *Different Transient Models – Limitations, advantages and disadvantages*, 28th Annual Meeting of PSIG (Pipeline Simulation Interest Group), San Francisco, California (1996).
[21] A. J. Osciadacz, *Simulation and Analysis of Gas Networks*, Gulf Publishing Company, Houston, (1987).
[22] E. Sekirnjak, *Transiente Technische Optimierung*, PSI Berlin, Technical Report, (2000).
[23] M. Steinbach, *On PDE Solution in Transient Optimization of Gas Networks*, Technical Report ZR-04-46, ZIB Berlin (2004).
[24] E. Truckenbrodt, *Fluidmechanik*, Bd. 1 & 2, Springer, Heidelberg, (1992).
[25] J. Zhou and M. A. Adewumi, *Simulation of transients in natural gas pipelines using hybrid TVD schemes*, Int. J. Numer. Meth. Fluids, 32 (2000), pp. 407–437.

Received September 15, 2004; revised February 2005.

E-mail address: `bandamk@ukzn.ac.za; herty@rhrk.uni-kl.de; klar@itwm.fhg.de`

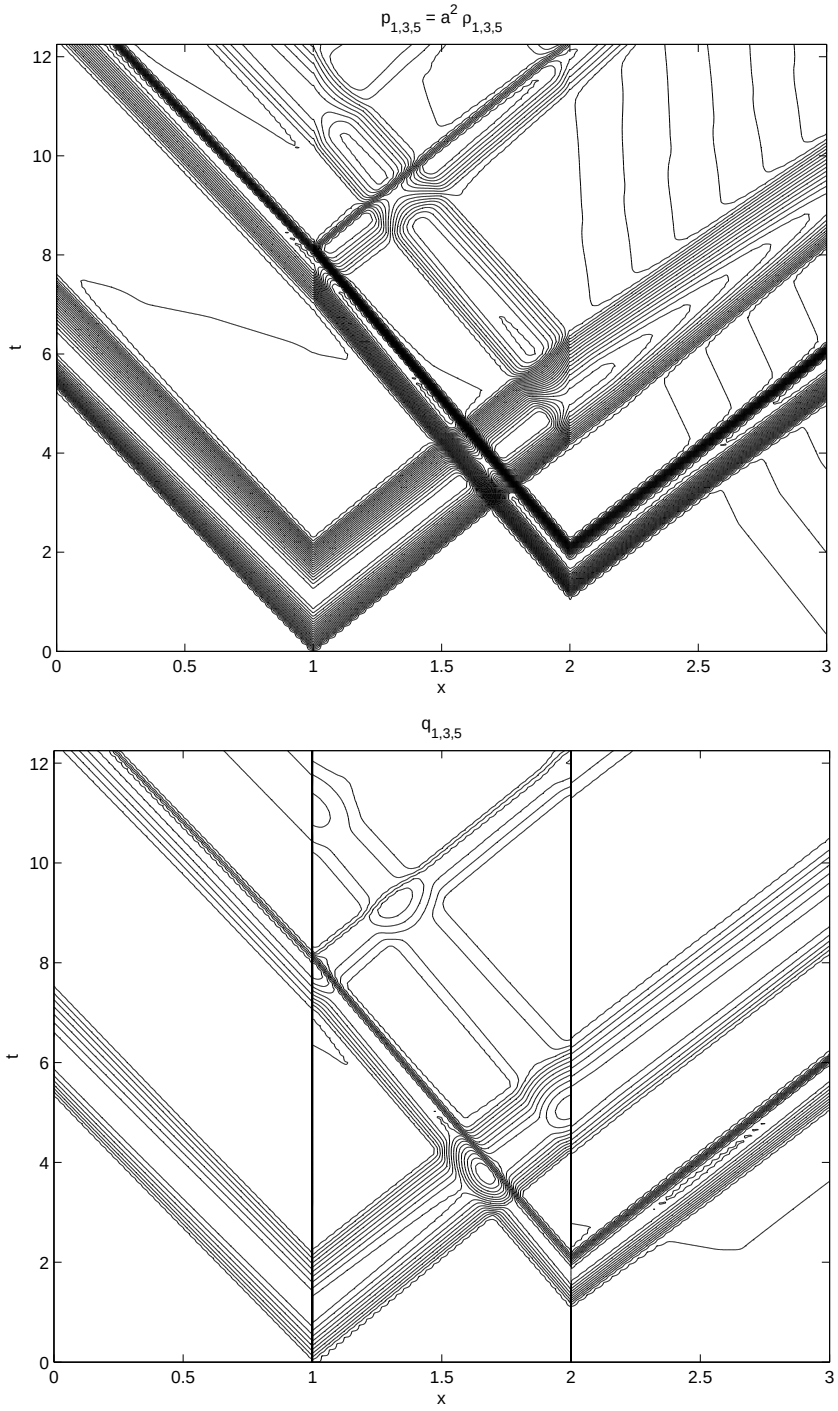

FIGURE 9. Contour lines of the pressures $a^2\rho_j$ (left) and the flux q_j (right) for pipes $j = 1, 3, 5$ for network of Figure 8

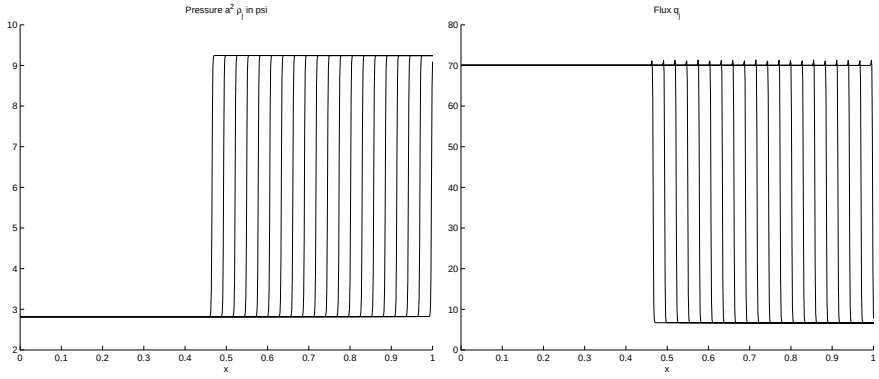

FIGURE 10. Simulation of a closed valve at $x = 1$ similar to [25]. Evolution of the pressure $a^2\rho_j$ (top) and the flux q_j (bottom) on pipe $j = 1$ up to time $t = 0.8$.